

Supplementary Tables

Supplementary Table 1: List of CH3 domain interface residues in the first chain (A) and their side chain contacting residues in the second chain (B)^a

<i>Interface Res. in Chain A</i>	<i>Contacting Residues in Chain B</i>
GLN A 347	LYS B 360'
TYR A 349	SER B 354' ASP B 356' GLU B 357' LYS B 360'
THR A 350	SER B 354' ARG B 355'
LEU A 351	LEU B 351' SER B 354' THR B 366'
SER A 354	TYR B 349' THR B 350' LEU B 351'
<i>ARG A 355</i>	THR B 350'
ASP A 356	TYR B 349' LYS B 439'
GLU A 357	TYR B 349' LYS B 370'
<i>LYS A 360</i>	GLN B 347' TYR B 349'
SER A 364	LEU B 368' LYS B 370'
THR A 366	LEU B 351' TYR B 407'
LEU A 368	SER B 364' LYS B 409'
LYS A 370	GLU B 357' SER B 364'
ASN A 390	SER B 400'
LYS A 392	ASP B 399' SER B 400' PHE B 405'
THR A 394	THR B 394' VAL B 397' PHE B 405' TYR B 407'
PRO A 395	VAL B 397'
VAL A 397	THR B 394' PRO B 395'
ASP A 399	LYS B 392' LYS B 409'
SER A 400	ASN B 390' LYS B 392'
PHE A 405	LYS B 392' THR B 394' LYS B 409'
TYR A 407	THR B 366' THR B 394' TYR B 407' LYS B 409'
LYS A 409	LEU B 368' ASP B 399' PHE B 405' TYR B 407'
LYS A 439	ASP B 356'

^aPositions involving interaction between oppositely charged residues are indicated in bold. Due to the 2-fold symmetry present in the CH3-CH3 domain interaction, each pairwise interaction is represented twice in the structure (for example, Asp A 356 --- Lys B 439' & Lys A 439 --- Asp B 356'; Figure 1). Eu numbering scheme is used here to identify residue positions.

Supplementary Table 2: Quantification of percentage of homodimer and heterodimer yields for the SDS-PAGE shown in Figure 2c^a

scFv-Fc	WT	D399'K	D399'K	D399'K;E356'K	D399'K;E357'K	D399'K;E356'K	D399'K;E357'K	T366'W (Hole)
Fc	WT	K409D;K360D	K409D; K392D	K409D;K392D	K409D;K392D	K409D;K439D	K409D;K370D	T366S;L368A; Y407V (Knob)
scFv-Fc / scFv-Fc	25.5	16.8	23.1	ND	ND	ND	ND	13.3
scFv-Fc / Fc	32.4	55.1	76.9	100	79.1	92.3	85.2	86.7
Fc / Fc	42.1	28.1	ND	ND	20.9	7.7	14.8	ND

^aND stands for Not Detectable in the density based analysis.

Supplementary Table 3: CH3-CH3 domain binding free energy for various mutants designed to enhance heterodimer formation, calculated using the EGAD program (1)^a

<i>Protein</i>	<i>Description</i>	ΔG (in <i>kcal/mol</i>)	$\Delta\Delta G_{mut}$ (in <i>kcal/mol</i>)	<i>Melting Temp.</i> T_m (in °C) ^b
WT	Wild Type	-30.69	0	80.4
T366W/Y407'A	Knob-Hole	-24.60	6.09	65.4
T366W/T366'S:L368'A:Y407'V	Knob-Hole	-28.57	2.12	69.4
K409D:K392D/D399'K:D356'K	Charge- Charge	-27.50	3.19	ND ^c

^aNot all possible charge-charge pairs were considered for the binding free energy calculation. Wild type is listed for comparison. ΔG is defined as energy difference between the complex and free states. The binding free energy of a mutant ($\Delta\Delta G_{mut}$) is defined as difference between the mutant (ΔG_{mut}) and wild type (ΔG_{WT}) free energies.

^bCH3 domain melting temperatures (T_m) for the knob-hole mutants and WT are as reported in the literature (2).

^cMelting temperature for the charge pair mutant was not measured using only the CH3 domain. The DSC profiles shown in the Supplementary Figure 4 includes CH3, CH2, and scFv domains.

Supplementary Figure Legends

Supplementary Figure 1. Flow chart of the scheme used to analyze the Fc crystal structures and sequences in order to arrive at the strategy (shown in Figure 1d) for engineering heterodimeric Fc.

Supplementary Figure 2. Structural conservation of the CH3 domain interface residues is shown here by superimposing the identified Fc crystal structures from the PDB. Only the side chain atoms of the interface residues are shown for clarity. The buried residues ($\%ASA \leq 10$) are colored based on atom type and the exposed residues ($\%ASA > 10$) are colored brown. The structurally not conserved residues are colored in green and their conformations in other structures are not shown for clarity.

Supplementary Figure 3. Multiple sequence alignment of (a) human and (b) mouse IgG subclasses' CH3 domain sequences. The star (*) indicates residue positions involved in the CH3-CH3 domain interaction identified based on the IgG1 human Fc crystal structure (1L6X). The CH3 domain interface charged residues marked with rectangles are highly conserved among the IgGs.

Supplementary Figure 4. Production of scFv-Fc/Fc heterodimers for Differential Scanning Calorimetric (DSC) analysis. (a) SDS-PAGE and western blot analysis of purified scFv-Fc/Fc heterodimer created using the charge pair strategy (K409D:K392D / D399'K:E356'K, lane 1), WT (lane 2), and the knobs-into-holes strategy

(T366W/T366'S:L368'A:Y407'V, lane 3) under reduced and non-reduced condition. Culture supernatants contain scFv-Fc/Fc heterodimers were first purified by Protein A affinity chromatography. To separate scFv-Fc/Fc heterodimer from contaminating homodimers for WT and knob-into-hole constructs, a 6xHis tag was placed at the C-terminal of the scFv-Fc construct. scFv-Fc/scFv-Fc homodimer and scFv-Fc/Fc heterodimer were separated from Fc/Fc homodimer by a nickel His-trap column and the scFv-Fc/Fc heterodimer was further purified by Size exclusion chromatography (SEC). **Left panel:** Western blot of scFv-Fc/Fc heterodimers preps after Protein A purification using anti-His antibody. Both WT and knob-into-hole constructs still contain scFv-Fc/scFv-Fc homodimer species. **Right panel:** SDS-PAGE analysis of purified scFv-Fc/Fc heterodimer after additional purification steps. (b) Differential Scanning Calorimetric (DSC) profiles for the three purified scFv-Fc/Fc constructs described in (a). DSC measurements were carried out for all samples at a concentration of 0.5mg/mL in pH 7.0 PBS buffer. Each sample was scanned at a rate of 0.25°C/min from 30 to 90°C. Reference scan using the PBS buffer was conducted and subtracted from the sample scans.

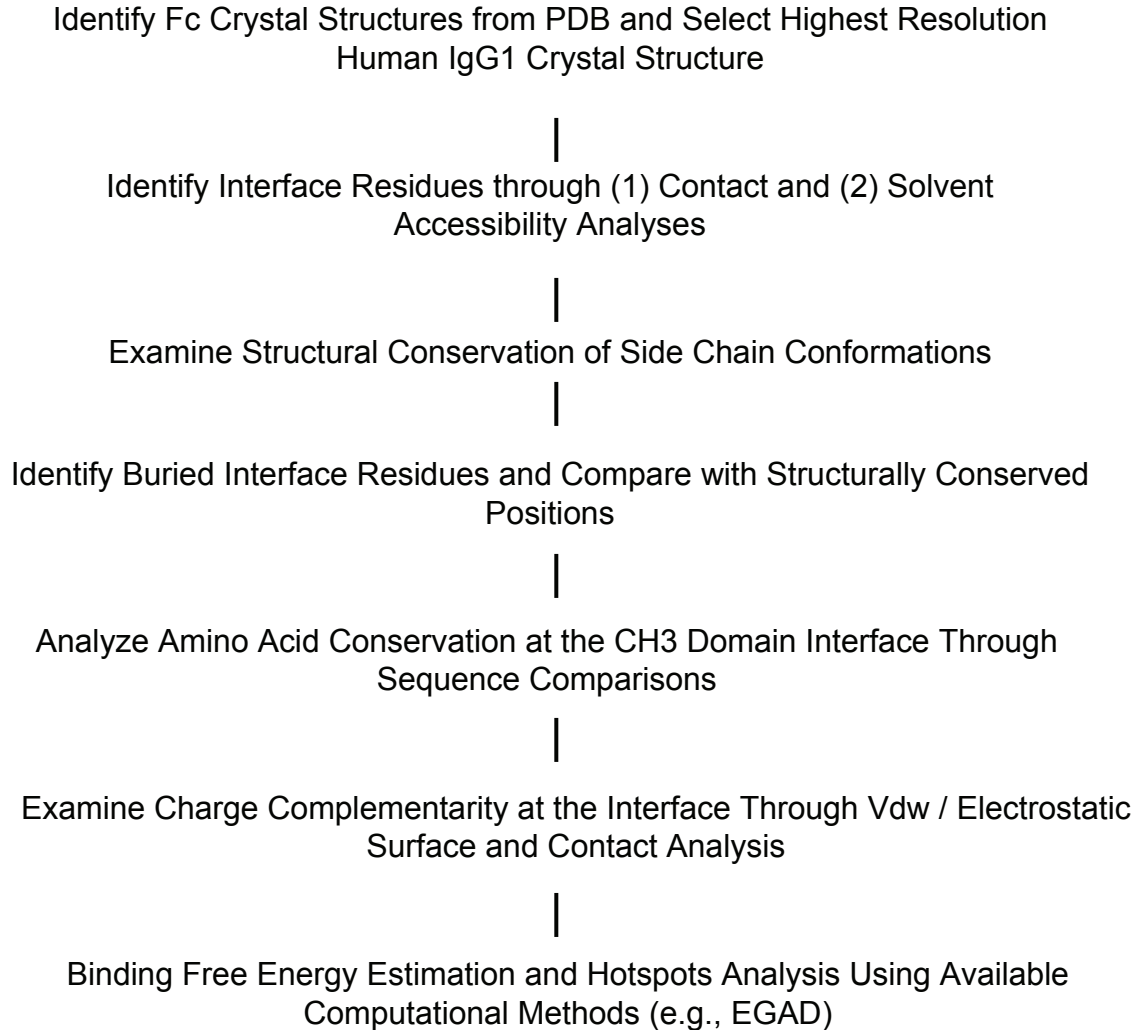
Supplementary Figure 5. Schematic diagram showing the potential products resulting from the co-expression of heavy chain and light chain-Fc fusion (a) without any mutations in the CH3 domain and (b) with charge pair mutations at the CH3 domain interface.

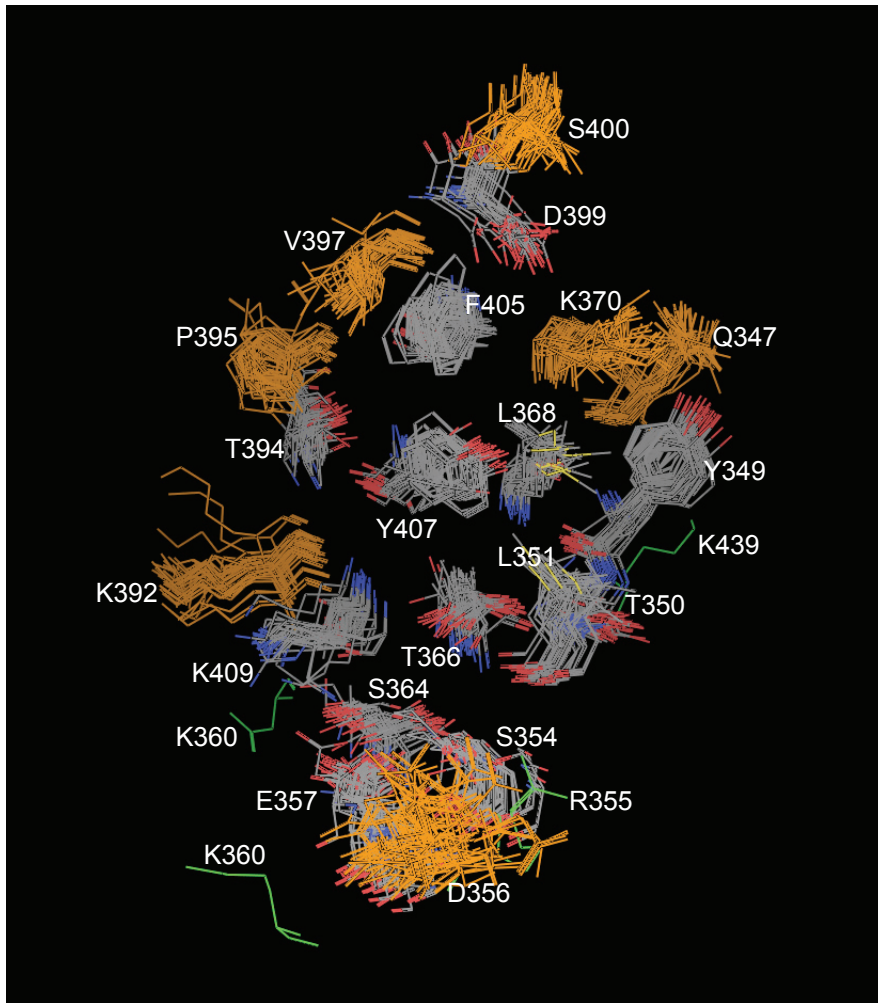
Supplementary Figure 6. Ribbon representation of the modeled heterodimeric CH3 domain structure showing the charge complementarity with (a) D399K mutation in the first chain and K392'D:K409'D mutations in the second chain and (b) D399K:E356K mutations in the first chain and K392'D:K409'D mutations in the second chain. Although both (a) and (b) design promote heterodimer formation, in the case of (a) the homodimer involving D399K mutation is not completely suppressed. The addition of E356K mutation away from the D399K mutation in the CH3 domain interface structural space, as shown in (b), leads to complete suppression of homodimers. However, the design (a) has higher thermal stability compared to the design (b).

Supplementary References

1. Pokala, N., and Handel, T. M. (2005) *J Mol Biol* **347**(1), 203-227
2. Atwell, S., Ridgway, J. B., Wells, J. A., and Carter, P. (1997) *J Mol Biol* **270**(1), 26-35

Computational Analyses Scheme





(a)

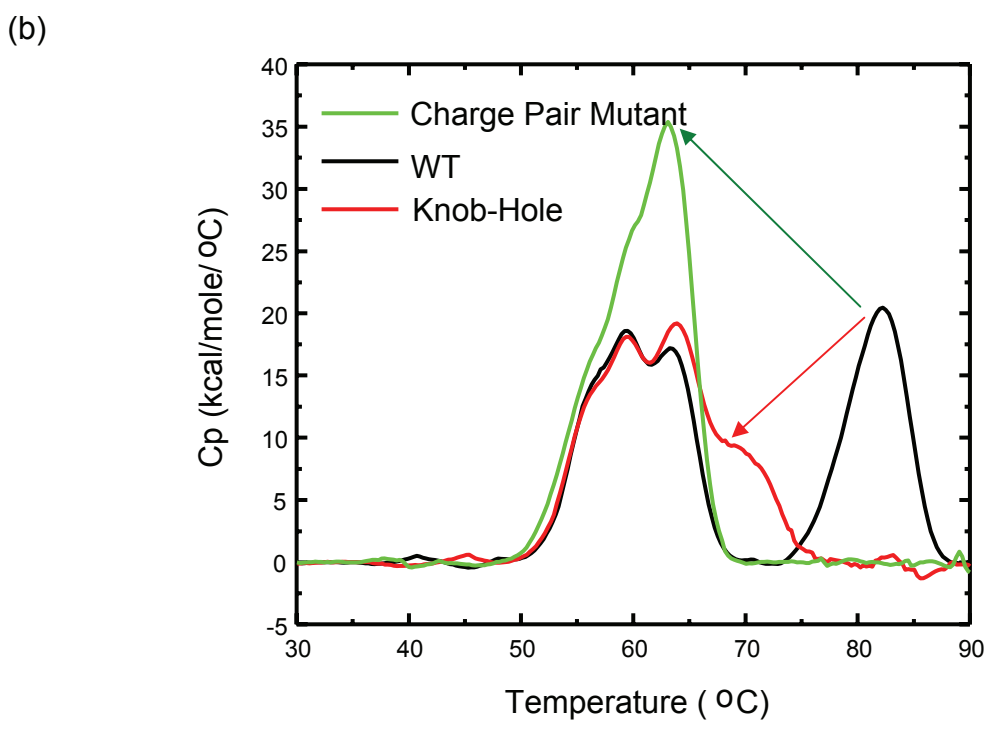
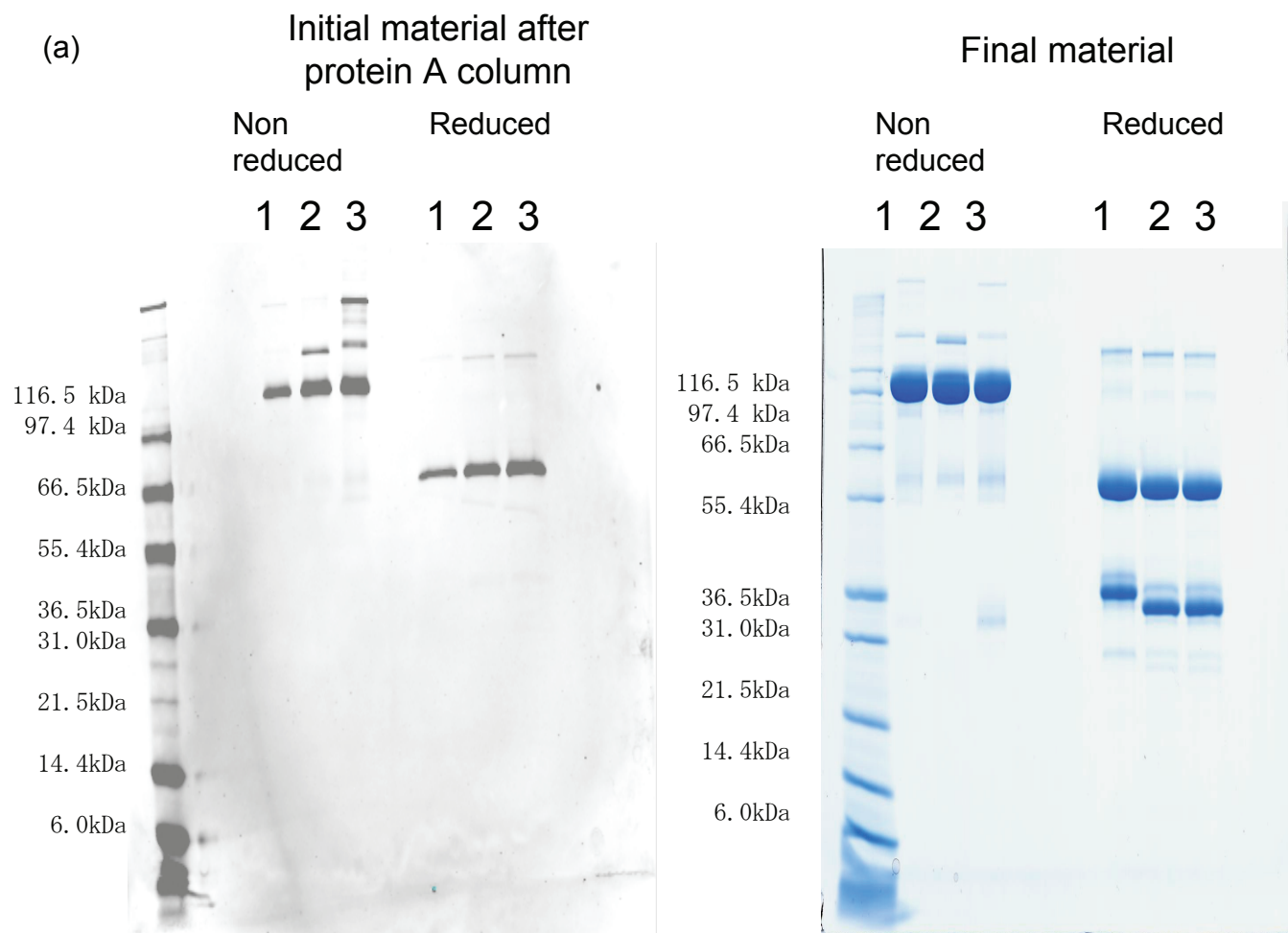
IGG1_HUMAN	AKGQPREPQVYITLPPSRDELTKNQVSLTCLVKGFYPSDIAVEWESNGQPENNYKTTTPPVL	390
IGG2_HUMAN	TKGQPREPQVYITLPPSRDEMTKKNQVSLTCLVKGFYPSDIAVEWESNGQPENNYKTTTPPML	
IGG3_HUMAN	TKGQPREPQVYITLPPSRDEMTKKNQVSLTCLVKGFYPSDIAVEWESNGQPENNYKTTTPPML	
IGG4_HUMAN	AKGQPREPQVYITLPPSRDEMTKKNQVSLTCLVKGFYPSDIAVEWESNGQPENNYKTTTPPVL	380
	AKGQPREPQVYITLPPSRDEMTKKNQVSLTCLVKGFYPSDIAVEWESNGQPENNYKTTTPPVL	370
	AKGQPREPQVYITLPPSRDEMTKKNQVSLTCLVKGFYPSDIAVEWESNGQPENNYKTTTPPVL	360
	AKGQPREPQVYITLPPSRDEMTKKNQVSLTCLVKGFYPSDIAVEWESNGQPENNYKTTTPPVL	350
	AKGQPREPQVYITLPPSRDEMTKKNQVSLTCLVKGFYPSDIAVEWESNGQPENNYKTTTPPVL	340

IGG1_HUMAN	DS DGSFFFLYSKLLTVDKSRWQQGNVFSCVMHEALHNHYTQKLSLSLSPGK	440
IGG2_HUMAN	DS DGSFFFLYSKLLTVDKSRWQQGNVFSCVMHEALHNHYTQKLSLSLSPGK	
IGG3_HUMAN	DS DGSFFFLYSKLLTVDKSRWQQGNVFSCVMHEALHNHYTQKLSLSLSPGK	430
IGG4_HUMAN	DS DGSFFFLYSRLTVDKSRWQEGNVFSCVMHEALHNHYTQKLSLSLSPGK	420
	DS DGSFFFLYSRLTVDKSRWQEGNVFSCVMHEALHNHYTQKLSLSLSPGK	410
	DS DGSFFFLYSRLTVDKSRWQEGNVFSCVMHEALHNHYTQKLSLSLSPGK	400

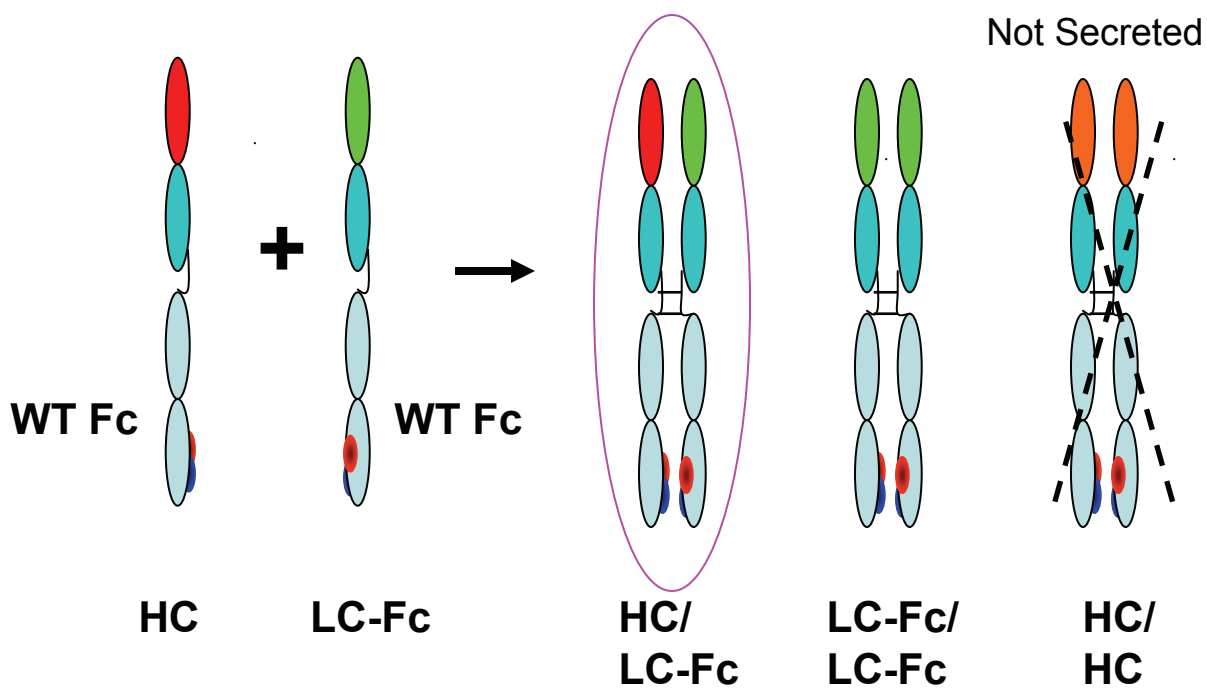
(b)

IGG1_HUMAN	AKGQPREPQVYITLPPSRDELTKNQVSLTCLVKGFYPSDIAVEWESNGQPENNYKTTTPPVL	
IGG1_MOUSE	TKGRPKAPQVYITLPPSRDEMTKKNQVSLTCLVKGFYPSDIAVEWESNGQPENNYKTTTPPVL	
IGG2A_MOUSE	PKGSVRAPQVYITLPPSRDEMTKKNQVSLTCLVKGFYPSDIAVEWESNGQPENNYKTTTPPVL	
IGG2B_MOUSE	IKGLVRAPQVYITLPPSRDEMTKKNQVSLTCLVKGFYPSDIAVEWESNGQPENNYKTTTPPVL	
IGG3_MOUSE	PKGRAQTPQVYITLPPSRDEMTKKNQVSLTCLVKGFYPSDIAVEWESNGQPENNYKTTTPPVL	

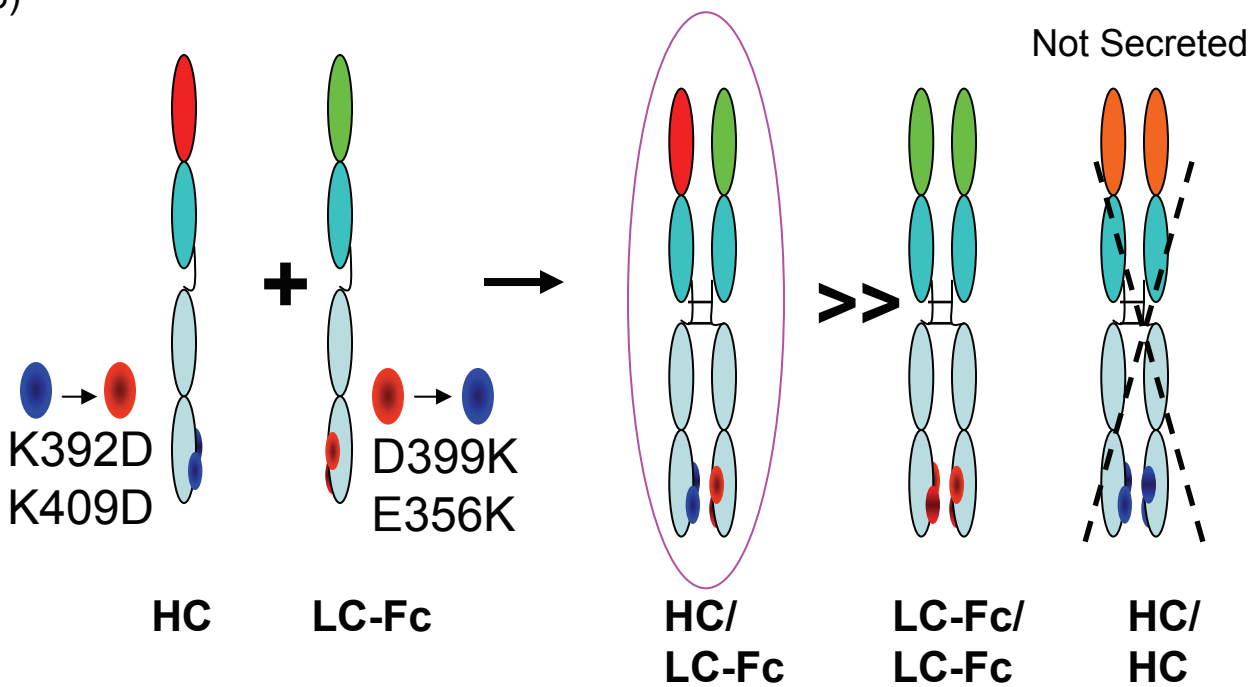
IGG1_HUMAN	DS DGSFFFLYSKLLTVDKSRWQQGNVFSCVMHEALHNHYTQKLSLSLSPGK	
IGG1_MOUSE	NTNGSYFVYSKLLTVDKSRWQQGNVFSCVMHEALHNHYTQKLSLSLSPGK	
IGG2A_MOUSE	DS DGSYFMYSKLLTVDKSRWQQGNVFSCVMHEALHNHYTQKLSLSLSPGK	
IGG2B_MOUSE	DS DGSYFIYSKLLTVDKSRWQQGNVFSCVMHEALHNHYTQKLSLSLSPGK	
IGG3_MOUSE	DS DGTGFVYSKLLTVDKSRWQQGNVFSCVMHEALHNHYTQKLSLSLSPGK	



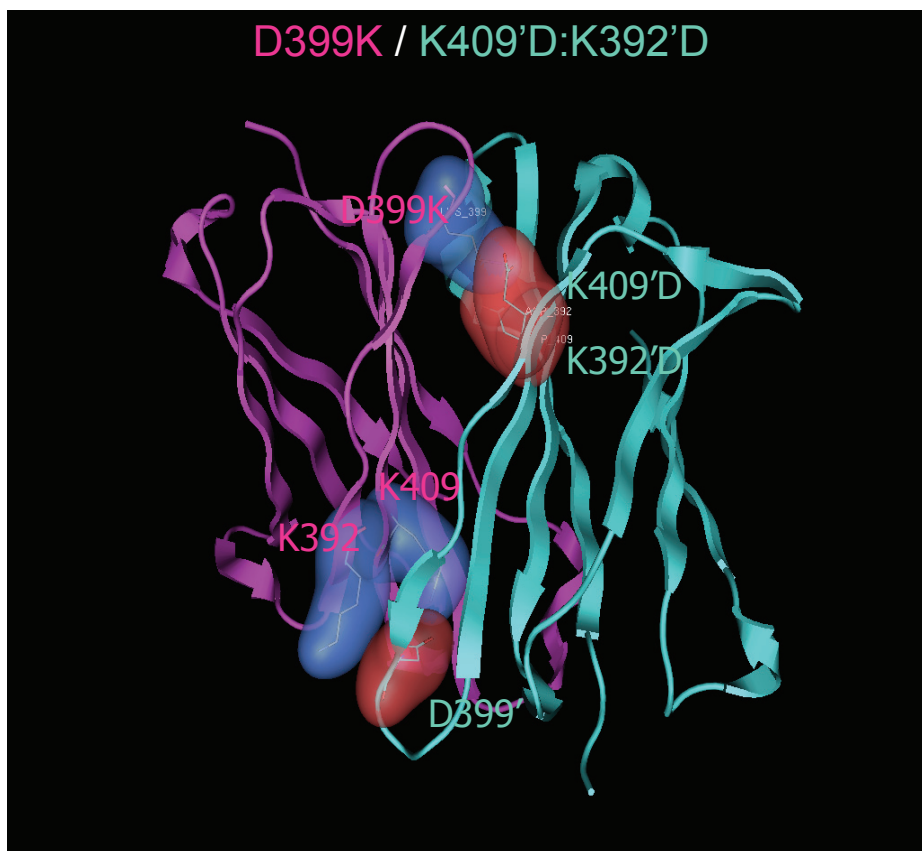
(a)



(b)



(a)



(b)

